

Proton Spectroscopic Factor in ${}^7\text{Li}$ from ${}^2\text{H}({}^6\text{He}, {}^7\text{Li})n$

Z. H. Li,* E. T. Li, B. Guo, X. X. Bai, Y. J. Li, S. Q. Yan, Y. B. Wang, G. Lian, J. Su, B. X. Wang, S. Zeng, X. Fang, and W. P. Liu
China Institute of Atomic Energy, P. O. Box 275(46), Beijing 102 413, P. R. China

The angular distribution of the ${}^2\text{H}({}^6\text{He}, {}^7\text{Li})n$ reaction was measured with a secondary ${}^6\text{He}$ beam of 36.4 MeV for the first time. The proton spectroscopic factor of ${}^7\text{Li}$ ground state was extracted to be 0.41 ± 0.05 by the normalization of the calculational differential cross sections with the distorted-wave Born approximation to the experimental data. It was found that the uncertainty of extracted spectroscopic factors from the one-nucleon transfer reactions induced by deuteron may be reduced by constraining the volume integrals of imaginary optical potentials.

PACS numbers: 21.10.Jx, 25.45.Hi, 25.60.Je, 25.70.Hi

I. INTRODUCTION

The essential constituents of nuclear shell model are the single particle orbits of the mean field which are occupied by protons and neutrons under Pauli principle. The spectroscopic factor describes the overlap between the initial and final states and yields the information on the occupancy of a given single particle orbit, which plays an important role in a variety of topics on nuclear reaction and nuclear astrophysics. Single nucleon transfer reactions such as (d, p) or (d, n) have been used extensively to extract the spectroscopic information of the single nucleon orbits in nuclei located at or near the stability line [1, 2, 3]. The spectroscopic study of exotic nuclei becomes feasible since the production of radioactive ion beams [4, 5, 6]. These measurements allow the extraction of the spectroscopic factors by normalizing the calculational differential cross sections with the distorted-wave Born approximation (DWBA) to the experimental ones at forward angles.

The $({}^7\text{Li}, {}^6\text{He})$ reaction is a valuable spectroscopic tool in the study of nuclear reactions because the shape of its angular distribution can be well reproduced by the DWBA calculations [7]. In the calculations of $({}^7\text{Li}, {}^6\text{He})$ reactions [7, 8, 9, 10, 11], the spectroscopic factor of ${}^7\text{Li}$ ground state was taken to be 0.59 given by Cohen and Kurath [12]. F. P. Brady et al. [13] extracted the spectroscopic factor of ${}^7\text{Li}$ ground state to be $S(p_{3/2}) = 0.62$ from the ${}^7\text{Li}(n, d){}^6\text{He}$ reaction with 56.3 MeV neutrons. L. Lapikás et al. [14] deduced the proton spectroscopic factor in ${}^7\text{Li}$ to be 0.42 ± 0.04 via the measurement of the ${}^7\text{Li}(e, e'p)$ reaction. This value is 32% smaller than that from the ${}^7\text{Li}(n, d){}^6\text{He}$ reaction. Thus, further measurement of the ${}^7\text{Li}$ spectroscopic factor is highly desired.

In the present work, the angular distribution of the ${}^2\text{H}({}^6\text{He}, {}^7\text{Li})n$ reaction was measured by using a secondary ${}^6\text{He}$ beam of 36.4 MeV, and analyzed with DWBA. The proton spectroscopic factor in ${}^7\text{Li}$ was then extracted and compared with the existing ones.

II. MEASUREMENT OF THE ANGULAR DISTRIBUTION

The experiment was carried out using the secondary beam facility [15, 16] of the HI-13 tandem accelerator, Beijing. A 46 MeV ${}^7\text{Li}$ primary beam from the tandem impinged on a 4.8 cm long deuterium gas cell at a pressure of about 1.5 atm. The front and rear windows of the gas cell are Havar foils, each in thickness of 1.9 mg/cm^2 . The ${}^6\text{He}$ ions were produced via the ${}^2\text{H}({}^7\text{Li}, {}^6\text{He}){}^3\text{He}$ reaction. After the magnetic separation and focus with a dipole and a quadruple doublet, a 37.6 MeV ${}^6\text{He}$ secondary beam was delivered and then collimated with a $\phi 7\text{-}\phi 5 \text{ mm}$ collimator complex. The ${}^6\text{He}$ beam was then recorded by a $23 \mu\text{m}$ thick silicon ΔE detector, which served as both particle identification and beam normalization. The typical purity and intensity of the ${}^6\text{He}$ beam are 99% and 3000 pps. The main contaminants were ${}^7\text{Li}$ ions out of Rutherford scattering of the primary beam in the gas cell windows as well as on the beam tube.

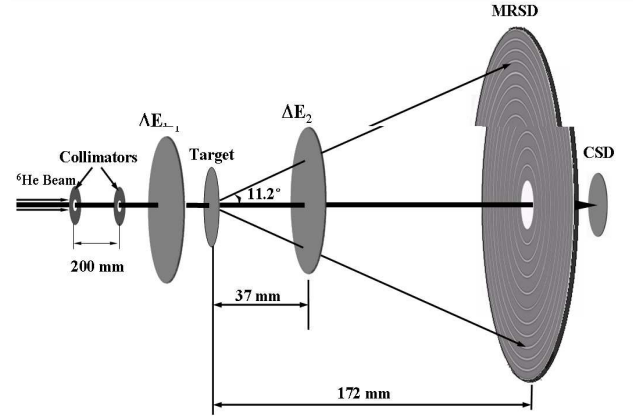


FIG. 1: Schematic layout of the experimental setup

The experimental setup is shown in Fig. 1. A $(\text{CD}_2)_n$ foil and a carbon foil, both in the thickness of 1.7 mg/cm^2 , were used as the targets to measure the ${}^2\text{H}({}^6\text{He}, {}^7\text{Li})n$ reaction and background, respectively. The energy of ${}^6\text{He}$ ions at the middle of the $(\text{CD}_2)_n$ was 36.4 MeV. A $300 \mu\text{m}$ thick multi-ring semiconductor de-

*Electronic address: zhli@ciae.ac.cn

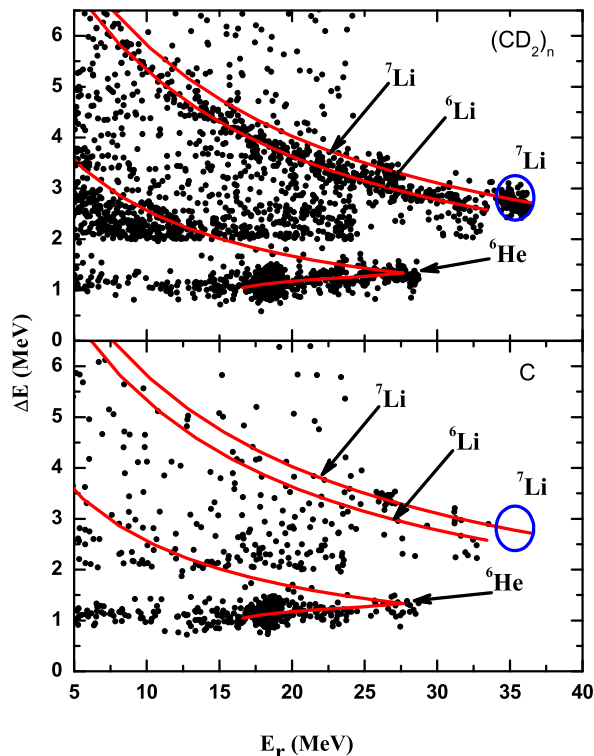


FIG. 2: (Color online) ΔE vs. E_r scatter plots of $(CD_2)_n$ target (top panel) and pure carbon target (bottom panel) measured by the fourth ring of MRSD. The red curves are the calculated ΔE vs. E_r for the particle identification of ${}^7\text{Li}$, ${}^6\text{Li}$ and ${}^6\text{He}$. The two-dimensional gate with blue color is the ${}^7\text{Li}$ kinematics region from the ${}^2\text{H}({}^6\text{He}, {}^7\text{Li})n$ reaction, corresponding to the fourth ring.

tector (MRSD) with center hole was used as a residue energy (E_r) detector which composed a $\Delta E - E_r$ counter telescope together with a $23 \mu\text{m}$ thick silicon ΔE detector and a $300 \mu\text{m}$ thick center silicon detector (CSD). Such a detector configuration covered the laboratory angular range from 0° to 11.2° , and the corresponding angular range in the center of mass frame for the ${}^2\text{H}({}^6\text{He}, {}^7\text{Li})n$ reaction was from 0° to 51.6° . Generally, the spectroscopic factor is extracted by fitting the theoretical calculations to the experimental data at the first peak in the angular distribution at forward angles [17], since the experimental angular distribution at the backward angles is more sensitive to the inelastic coupling effects and other high-order ones, which can not be well described theoretically. The DWBA calculation predicts that the first peak of the angular distribution for the ${}^2\text{H}({}^6\text{He}, {}^7\text{Li})n$ reaction is around 20° in the center of mass frame, thus the present setup is propitious to the extraction of the ${}^7\text{Li}$ spectroscopic factor.

The accumulated quantity of incident ${}^6\text{He}$ was approximately 2.71×10^8 for the $(CD_2)_n$ target measurement, and 8.41×10^7 for background measurement with the carbon target. As an example, Fig. 2 displays the $\Delta E - E_r$ scatter plots of both $(CD_2)_n$ and carbon tar-

gets for the fourth ring of MRSD. For the sake of saving CPU time in dealing with the experimental data, we set a cut at $\Delta E = 2.0$ MeV. All the events below the cut were scaled down by a factor of 100, while the ${}^7\text{Li}$ events remain unchanged. The red curves in Fig. 2 are the calculated ΔE vs. E_r for ${}^7\text{Li}$, ${}^6\text{Li}$ and ${}^6\text{He}$, respectively. The two-dimensional gate with blue color is the ${}^7\text{Li}$ kinematics region from the ${}^2\text{H}({}^6\text{He}, {}^7\text{Li})n$ reaction, corresponding to the fourth ring. The ${}^7\text{Li}$ events can be clearly identified in this figure. We didn't find any ${}^7\text{Li}$ event in the gate for the background runs. The measured angular distribution is given in Fig. 3. The uncertainties of differential cross sections mainly arise from the statistics and the assignment of ${}^7\text{Li}$ kinematics regions.

III. DWBA CALCULATIONS

The angular distribution measured in this work includes the contributions of the ground and first excited states in ${}^7\text{Li}$ populated by the ${}^2\text{H}({}^6\text{He}, {}^7\text{Li})n$ reaction. The events of these two states can not be separated because their energy difference is only 0.48 MeV which is less than the energy spread (0.62 MeV) of the ${}^6\text{He}$ beam.

The ${}^2\text{H}({}^6\text{He}, {}^7\text{Li})n$ reaction leading to the ground state of ${}^7\text{Li}$ is a $(3/2^-, 1/2) \rightarrow (0^+, 1)$ transition. Parity and angular momentum considerations dictate that only $1p_{3/2}$ pickup is possible. In the same way, the ${}^2\text{H}({}^6\text{He}, {}^7\text{Li}^*)n$ reaction leading to the first excited state of ${}^7\text{Li}$ is a $(1/2^-, 1/2) \rightarrow (0^+, 1)$ transition and only $1p_{1/2}$ pickup contributes to the reaction. The relationship among the experimental differential cross sections, the DWBA calculations and the spectroscopic factors can be expressed as

$$\left(\frac{d\sigma}{d\Omega}\right)_{exp} = S_d S_{\tau Li} \left(\frac{d\sigma}{d\Omega}\right)_{gs} + S_d S_{\tau Li^*} \left(\frac{d\sigma}{d\Omega}\right)_{ex1}, \quad (1)$$

where $\left(\frac{d\sigma}{d\Omega}\right)_{exp}$ is the experimental differential cross section, $\left(\frac{d\sigma}{d\Omega}\right)_{gs}$ and $\left(\frac{d\sigma}{d\Omega}\right)_{ex1}$ are the calculational differential cross sections for the ${}^2\text{H}({}^6\text{He}, {}^7\text{Li})n$ and ${}^2\text{H}({}^6\text{He}, {}^7\text{Li}^*)n$ reactions. S_d is the spectroscopic factor for $d \rightarrow p + n$, which is derived to be 0.859 from Ref. [18]. $S_{\tau Li}$ and $S_{\tau Li^*}$ are the proton spectroscopic factors of the ground and first excited states in ${}^7\text{Li}$. According to the translationally invariant shell model [19] calculation with the code DESNA [20], and Boyarkina's wave function tables [21], the ratio of $S_{\tau Li}/S_{\tau Li^*}$ is 1.0 [22]. Thus, the proton spectroscopic factors in ${}^7\text{Li}$ can be extracted through Eq. (1) by the normalization of DWBA calculations to the experimental data.

The code FRESKO [23] was used to compute the angular distribution of the ${}^2\text{H}({}^6\text{He}, {}^7\text{Li})n$ reaction leading to the ground and first excited states of ${}^7\text{Li}$. Following our previous work in Ref. [24], the effective deuteron potential was calculated with the adiabatic model of Johnson and Soper [25, 26]. The optical potential parameters for the nucleon-nucleus were derived by the CH89 global

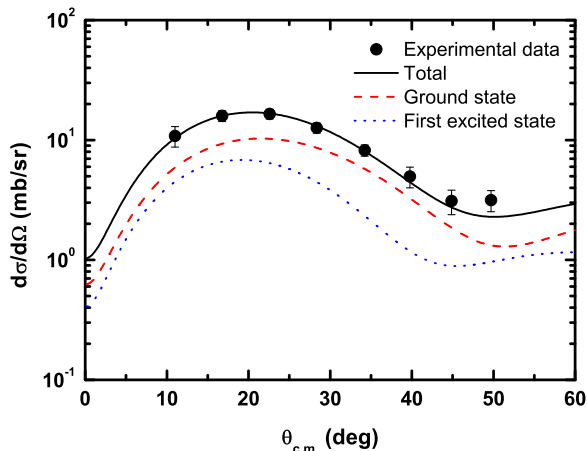


FIG. 3: (Color online) Angular distribution of the ${}^2\text{H}({}^6\text{He}, {}^7\text{Li})n$ reaction.

systematics [27]. The parameterization was based on the understanding of the optical potential theory, such as the folding model and nuclear matter approaches instead of determining the optical potentials phenomenologically. Up to 300 angular distributions and 9000 data points of proton and neutron differential cross sections were involved in the extensive database. The optical potentials derived in this way have been successfully used in the DWBA calculations for the (d, p) reaction on light nuclei [3, 17, 24]. The optical potential parameters for the entrance and exit channels used in our calculations, denoted as D1 and N1 respectively, are listed in Table I. Five data points in the first peak of the experimental angular distribution were used to extract the spectroscopic factors in the DWBA calculations. The normalized angular distributions are presented in Fig. 3 together with the experimental data. The dashed and dotted lines are respectively the calculated angular distributions for ${}^2\text{H}({}^6\text{He}, {}^7\text{Li})n$ leading to the ground and first excited states in ${}^7\text{Li}$, and the solid line with black color is the total angular distribution. One can see that the shape of the experimental angular distribution is well reproduced. ${}^7\text{Li}$ proton spectroscopic factor deduced from the present experimental data is 0.40 ± 0.02 . The error is only caused by the uncertainty of the five data points in the first peak of the measured angular distribution.

IV. THE UNCERTAINTY ANALYSIS

In general, the uncertainties of the extracted spectroscopic factor by the DWBA calculations originate from the ambiguity of the optical potential parameters for both the entrance and exit channels, and that of binding potential parameters in the bound state. The optical potential parameters for nucleon-nucleus in Refs. [27, 28, 29, 30, 31, 32] were used in the present calculations, and it is found that the potential parameters taken

TABLE I: Optical potential parameters used in DWBA calculations, where V , W are in MeV, r and a are in fm, the geometrical parameters of single particle bound state are set to be $r_0 = 1.25$ fm and $a = 0.65$ fm.

Set No.	D1	D2	D3	D4	D5	N1
V	97.79	86.32	76.41	86.80	80.53	41.54
r_v	1.13	1.17	1.25	1.13	1.15	1.41
a_v	0.72	0.73	0.77	0.80	0.81	0.50
W_V	2.05	0.18				
W_D	13.91	12.33	13.0	12.0	17.31	13.58
r_w	1.10	1.325	1.25	1.56	1.34	1.35
a_w	0.72	0.66	0.65	0.68	0.68	0.20
V_{so}	5.90	6.98	6.0	5.2		5.50
r_{so}	0.68	1.07	1.25	0.85		1.15
a_{so}	0.63	0.66	0.77	0.48		0.50
r_c	1.30	1.30	1.30	1.30	1.15	
Ref.	[26]	[33]	[34]	[35]	[31]	[27]

from the CH89 global systematics can give a best fit in the first peak of the ${}^6\text{He}(d, n){}^7\text{Li}$ angular distribution. In order to study the uncertainties of the spectroscopic factor associated with the various ${}^6\text{He} + d$ optical potentials, we used the additional four sets of ${}^6\text{He} + d$ potential parameters to extract the proton spectroscopic factor of ${}^7\text{Li}$. They are labeled as D2, D3, D4 and D5 respectively, as listed in Table I. Set D2 is obtained from the analysis of an extensive set of data [33], which includes the results of both polarized and unpolarized elastic deuteron scattering on the nuclei from ${}^{27}\text{Al}$ to ${}^{238}\text{Th}$ in the energy range of $E_d = 12 - 90$ MeV. Recently, the expression for D2 has been extrapolated to the nuclei of $A < 27$ [17]. Set D3 is based on the analysis of the elastic scattering of 52 MeV deuterons from 27 nuclei [34]. Set D4 is deduced from the elastic scattering of 30 MeV polarized deuterons from 10 nuclei [35]. Set D5 is the deuteron global potential for the nuclei of $Z \geq 12$ with deuteron energies from 12 to 25 MeV [31]. As a comparison, Fig. 4 shows the angular distributions calculated with all the five sets of the deuteron optical potentials together with the present experimental data. One can see that the experimental angular distribution is fairly reproduced by all the five sets of optical potentials. The extracted spectroscopic factors are 0.40, 0.37, 0.36, 0.45 and 0.46, respectively. Their average is 0.41 with a standard deviation of 0.05.

In order to estimate the uncertainty of the spectroscopic factor from the potential of ${}^6\text{He} + p$ bound state in ${}^7\text{Li}$, we have tested the influence of the geometrical parameters (r_0 and a) on the spectroscopic factor. The radius was changed from 1.10 to 1.40 fm while the diffuseness was adjusted to reproduce the rms radius of the valence proton in ${}^7\text{Li}$ which was calculated with the charge rms radii of ${}^6\text{He}$ and ${}^7\text{Li}$ in Refs. [36, 37] according to

$$r_{{}^7\text{Li}}^2 = \frac{1}{Z+1} (Zr_{{}^6\text{He}}^2 + r_p^2 + \frac{Z}{Z+1} r_v^2), \quad (2)$$

where $r_{{}^7\text{Li}}$, $r_{{}^6\text{He}}$ and r_p are the charge rms radii for ${}^7\text{Li}$, ${}^6\text{He}$ and proton, respectively. r_v is the rms radius of the

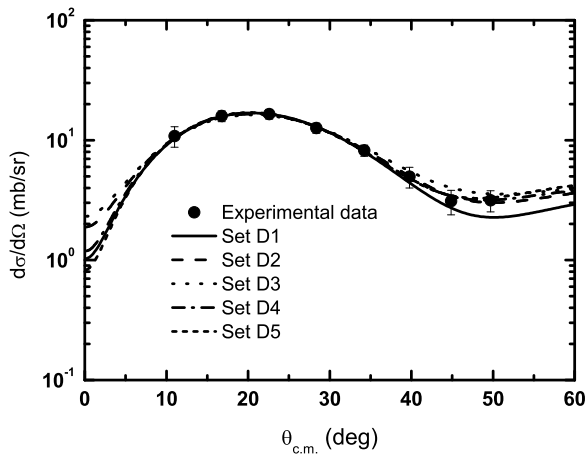


FIG. 4: Comparison of the angular distributions of ${}^2\text{H}({}^6\text{He}, {}^7\text{Li})n$ with 5 sets of optical potential parameters.

valence proton in ${}^7\text{Li}$, Z denotes the proton number in ${}^6\text{He}$. The above changes led to a 3% uncertainty of the deduced spectroscopic factor, which was negligible compared with the uncertainty from deuteron- ${}^6\text{He}$ potential parameters. The final value of the proton spectroscopic factor in ${}^7\text{Li}$ is 0.41 ± 0.05 . The error is from the measurement (5%) and the uncertainties of optical potential parameters (11%).

Figure 5 shows the comparison of ${}^7\text{Li}$ spectroscopic factors from theoretical calculations and experiments. The ${}^7\text{Li}$ spectroscopic factor obtained in our work is smaller than the theoretical calculations reported in Refs. [12] and [38]. Comparing with the experimental results, ours is 34% smaller than that extracted from the ${}^7\text{Li}(n, d){}^6\text{He}$ reaction [13], and in good agreement with those from the ${}^7\text{Li}(e, e'p)$ reaction by L. Lapikás et al. [14] and the ${}^7\text{Li}(d, {}^3\text{He}){}^6\text{He}$ reaction by A. H. Wuosmaa et al. [39] very recently.

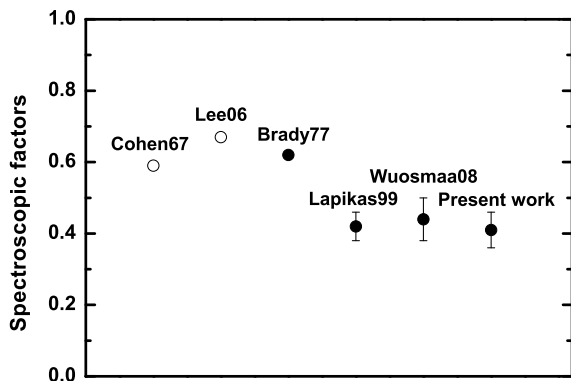


FIG. 5: Comparison of spectroscopic factors for ${}^7\text{Li}(3/2^-) \rightarrow {}^6\text{He} + p$. The solid and open circles represent the experimental and theoretical results respectively.

V. CONCLUSION AND DISCUSSION

The ${}^2\text{H}({}^6\text{He}, {}^7\text{Li})n$ angular distribution was measured with a secondary ${}^6\text{He}$ produced by the secondary beam facility of HI-13 tandem accelerator in Beijing. The proton spectroscopic factor in ${}^7\text{Li}$ ground state is extracted to be 0.41 ± 0.05 , which is in good agreement with those from the ${}^7\text{Li}(e, e'p)$ reaction [14] and the ${}^7\text{Li}(d, {}^3\text{He}){}^6\text{He}$ reaction [39].

The error (12%) of the spectroscopic factor given in our work mainly arises from the uncertainty (11%) of the optical potentials. Thus it is important to further investigate the influence of optical potentials. It is found that the volume integrals for the real part of five sets potentials only differ by a factor of 3%, while those for the imaginary part deviate up to 20%. The uncertainty of the spectroscopic factor mainly arises from the uncertainty of the imaginary optical potentials. We found a linear relationship between the volume integrals of the imaginary part and the spectroscopic factors, as shown in Fig. 6. Therefore, the uncertainty of the extracted spectroscopic factors can be reduced by constraining the imaginary volume integral for deuteron-nucleus correctly. Generally speaking, the angular distribution of the elastic scattering can provide fairly good information on the real part of the optical potential. However, it can only give relatively poor information on the imaginary part of the optical potential. Consequently, it is of importance for extracting the imaginary potential parameters to study the deuteron-nucleus reactions other than elastic scattering.

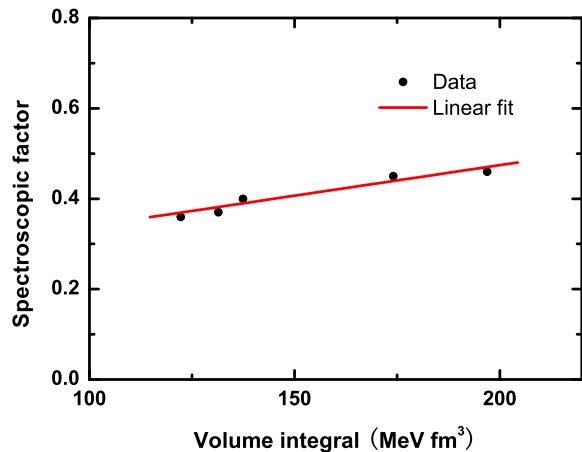


FIG. 6: (Color online) Spectroscopic factors as a function of the volume integral for the imaginary part of the optical potential parameters. The red line is a linear fit of the data points.

Acknowledgments

This work is supported by the National Basic Research Programme of China under Grant No. 2007CB815003,

the National Natural Science Foundation of China under Grant Nos. 10675173, 10705053 and 10735100.

-
- [1] M. H. Macfarlane and J. B. French, *Rev. Mod. Phys.* **32**, 567 (1960).
- [2] M. Assunção, R. Lichtenthäler, A. Lépine-Szily, G. F. Lima, and A. M. Moro, *Phys. Rev. C* **70**, 054601 (2004).
- [3] M. B. Tsang, J. Lee, and W. G. Lynch, *Phys. Rev. Lett.* **95**, 222501 (2005).
- [4] Z. H. Li, W. P. Liu, X. X. Bai, B. Guo, G. Lian, S. Q. Yan, B. X. Wang, S. Zeng, Y. Lu, J. Su, et al., *Phys. Rev. C* **71**, 052801 (2005).
- [5] A. H. Wuosmaa, K. E. Rehm, J. P. Greene, D. J. Henderson, R. V. F. Janssens, C. L. Jiang, L. Jisonna, E. F. Moore, R. C. Pardo, M. Paul, et al., *Phys. Rev. Lett.* **94**, 082502 (2005).
- [6] Z. H. Li, B. Guo, S. Q. Yan, G. Lian, X. X. Bai, Y. B. Wang, S. Zeng, J. Su, B. X. Wang, W. P. Liu, et al., *Phys. Rev. C* **74**, 035801 (2006).
- [7] K. W. Kemper, R. L. White, L. A. Charlton, G. D. Gunn, and G. E. Moore, *Phys. Lett. B* **52**, 179 (1974).
- [8] R. L. White and K. W. Kemper, *Phys. Rev. C* **10**, 1372 (1974).
- [9] J. E. Kim and W. W. Daehnick, *Phys. Rev. C* **23**, 742 (1981).
- [10] K. W. Kemper, G. E. Moore, R. J. Puigh, and R. L. White, *Phys. Rev. C* **15**, 1726 (1977).
- [11] M. E. Williams-Norton, G. M. Hudson, K. W. Kemper, G. E. Moore, G. A. Norton, R. J. Puigh, and A. F. Zeller, *Phys. Rev. C* **12**, 1899 (1975).
- [12] S. Cohen and D. Kurath, *Nucl. Phys. A* **101**, 1 (1967).
- [13] F. P. Brady, N. S. P. King, B. E. Bonner, M. W. McNaughton, J. C. Wang, and W. W. True, *Phys. Rev. C* **16**, 31 (1977).
- [14] L. Lapikás, J. Wesseling, and R. B. Wiringa, *Phys. Rev. Lett.* **82**, 4404 (1999).
- [15] X. Bai, W. Liu, J. Qin, Z. Li, S. Zhou, A. Li, Y. Wang, Y. Cheng, and W. Zhao, *Nucl. Phys. A* **588**, 273c (1995).
- [16] W. P. Liu, Z. H. Li, X. X. Bai, Y. B. Wang, G. Lian, S. Zeng, S. Q. Yan, B. X. Wang, Z. X. Zhao, T. J. Zhang, et al., *Nucl. Instrum. Methods Phys. Res. B* **204**, 62 (2003).
- [17] X. D. Liu, M. A. Famiano, W. G. Lynch, B. Tsang, and J. A. Tostevin, *Phys. Rev. C* **69**, 064313 (2004).
- [18] L. D. Blokhintsev, I. Borbely, and E. I. Dolinskii, *Sov. J. Part. Nucl.* **8**, 485 (1977).
- [19] Y. F. Smirnov and Y. M. Tchuivil'sky, *Phys. Rev. C* **15**, 84 (1977).
- [20] A. T. Rudchik and Y. M. Tchuivil'sky, *Ukrainian Journal of Physics* **30**, 819 (1985).
- [21] A. N. Boyarkina, *Structure of 1p-shell nuclei, Moscow State University report* (1973).
- [22] A. A. Rudchik, A. T. Rudchik, G. M. Kozeratska, O. A. Ponkratenko, E. I. Koshchy, A. Budzanowski, B. Czech, S. Kliczeski, R. Siudak, I. Skwirezyńska, et al., *Phys. Rev. C* **72**, 034608 (2005).
- [23] I. J. Thompson, *Comput. Phys. Rep.* **7**, 167 (1988).
- [24] B. Guo, Z. H. Li, W. P. Liu, and X. X. Bai, *J. Phys. G: Nucl. Part. Phys.* **34**, 103 (2007).
- [25] G. R. Satchler, *Phys. Rev. C* **4**, 1485 (1971).
- [26] G. L. Wales and R. C. Johnson, *Nucl. Phys. A* **274**, 168 (1976).
- [27] R. L. Varner, W. J. Thompson, T. L. McAbee, E. J. Ludwig, and T. B. Clegg, *Phys. Rep.* **201**, 57 (1991).
- [28] B. A. Watson, P. P. Singh, and R. E. Segel, *Phys. Rev.* **182**, 977 (1969).
- [29] F. D. Bechetti, Jr., and G. W. Greenless, *Phys. Rev.* **182**, 1190 (1969).
- [30] J. J. H. Menet, E. E. Gross, J. J. Malanify, and A. Zucker, *Phys. Rev. C* **4**, 1114 (1971).
- [31] C. M. Perey and F. G. Perey, *Atomic data and nuclear data tables* **17**, 1 (1976).
- [32] J. P. Jeukenne, A. Lejeune, and C. Mahaux, *Phys. Rev. C* **15**, 10 (1977).
- [33] W. W. Daehnick, J. D. Childs, and Z. Vrcelj, *Phys. Rev. C* **21**, 2253 (1980).
- [34] F. Hinterberger, G. Mairle, U. Schmidt-Rohr, and G. J. Wagner, *Nucl. Phys. A* **111**, 265 (1968).
- [35] G. Perrin, N. V. Sen, J. Arvieux, R. Darves-Blanc, J. L. Durand, A. Fiore, J. C. Gondrand, F. Merchez, and C. Perrin, *Nucl. Phys. A* **282**, 221 (1977).
- [36] I. Tanihata, H. Hamagaki, O. Hashimoto, Y. Shida, N. Yoshikawa, K. Sugimoto, O. Yamakawa, T. Kobayashi, and N. Takahashi, *Phys. Rev. Lett.* **55**, 2676 (1985).
- [37] C. Forssén, E. Caurier, and P. Navrátil, *Phys. Rev. C* **79**, 021303(R) (2009).
- [38] J. Lee, J. A. Tostevin, B. A. Brown, F. Delaunay, W. G. Lynch, M. J. Saelim, and M. B. Tsang, *Phys. Rev. C* **73**, 044608 (2006).
- [39] A. H. Wuosmaa, J. P. Schiffer, K. E. Rehm, J. P. Greene, D. J. Henderson, R. V. F. Janssens, C. L. Jiang, L. Jisonna, J. C. Lighthall, S. T. Marley, et al., *Phys. Rev. C* **78**, 041302(R) (2008).